BARKSDALE, R., ROBNETT, Q. and LAI, J.
Georgia Institute of Technology, Atlanta, Georgia, USA
ZEEVAERT-WOLFF, A.
Consultant, Mexico City, Mexico

Experimental and Theoretical Behavior of Geotextile Reinforced Aggregate Soil Systems

Comportement expérimental et théorique des systèmes agrégats-sol renforcés de géotextiles

The development is briefly described of a general finite element computer program for analyzing a plane strain or axisymmetric fabric reinforced soil continuum. The results are also described of an extensive series of model tests conducted in 0.9 and 2.5 m dia. circular test tanks simulating an aggregate surfaced haul road. Fabric reinforcement was found to be effective in reducing rutting partly by changing the state of stress in the soft clay subgrade. After large rut depths develop, measured vertical stresses in fabric reinforced systems on the centerline beneath the load averaged about 83% of Boussinesq stresses compared to 88% for a nonfabric system. Fabric reinforcement caused a substantial reduction in permanent strain (and hence rutting) in the soft clay subgrade for a depth equal to about one loading diameter. Other consequences of fabric reinforcement are also discussed.

Le mémoire décrit brièvement le developpement d'un programme à l'ordinateur, composé des éléments finis généraux, pour l'analyse d'une déformation plane ou d'un continuum axisymmétrique du sol renforcé par un tissu. On présente en outre les résultats d'une série étendue d'éssais en modèle, dans lesquels on a simulé une route de camionnage en employant des cuves d'éssai circulaires aux diametres de 0.9 m et de 2.5 m. Les éssais montrent que le tissu affaiblit effectivement le sillonage, en partie à cause d'un changement de l'état de resistance dans le sous-sol d'argile tendre. Après l'apparence des ornières assez profondes, les résistances verticales measurées sur le trait de centre sous la charge, dans les systèmes renforcés en textile, donnent une moyenne à peu près 83% des résistances Boussinesq, par rapport à 88% dans les systèmes sans tissu. Le renforcement en textile suscite une diminution importante de la déformation permanente (et, par consequent, du sillonage d'ornières) dans le sous-sol d'argile tendre, jusqu'à la profondeur approximative d'un diamètre de charge. Le menoire traite aussi d'autres suites du renforcement textile.

INTRODUCTION

At the present time relatively little research has been undertaken to define the basic mechanisms which control the performance of fabrics in geotechnical applications. An understanding of the mechanics of fabric reinforcement in this type application is required to develop rational design procedures compatible with the actual mechanics of fabric reinforcement behavior.

This paper describes the development of a general analytical model for fabric reinforced continuum problems, and summarizes some of the findings of an extensive series of model tests conducted in 0.9 m and 2.5 m (3 ft. and 8 ft.) dia. circular tanks. Although the GAPPS7 finite element program developed is quite general, the verification and parametric studies presented are limited to haul road applications.

FINITE ELEMENT MODEL

Introduction. The GAPPS7 finite element program accurately models a layered soil continuum reinforced with fabric and subjected to multiple load applications (1,2). Additional important features of the GAPPS7 program include (1) the ability to consider either small or large displacements which occur under multiple wheel loadings in a haul road, (2) modeling of materials exhibiting stress dependent behavior including elastic, plastic and failure response, (3) modeling of the fabric interfaces including provisions for slip or separation, (4) a two-dimensional flexible fabric membrane element not capable of taking either bending or compression loading, (5) no-tension analysis for granular materials, and (6) provision for solving either plane strain or axisymmetric problems. The GAPPS7 program does not consider either inertia forces or creep, and repetitive loadings are applied at a stationary position (i.e., it does not move along the continuum). Material properties can, however, be changed for each loading cycle to consider time and/or load dependent changes in properties.

To make the GAPPS7 program practical for routine use, an automatic data generation program MESHG4 was developed. In addition to handling material properties, MESHG4 completely generates the finite element mesh from a minimum of input data. To check the generated mesh and assist in interpreting the large quantity of data generated by GAPPS7, a plot program was developed called PTMESH. Use of these programs greatly facilitates performing finite element analyses and also checking for errors in the data.

For a typical 44 to 56 element mesh the computer running times vary from about 500 to 750 system seconds on the CDC CYBER 74 computer; actual cost is about $10 to $12 (U.S.) for an economy run. The running times and costs are for nonlinear material properties, 8 to 10 load increments, and the small displacement option.

Eight Node Isoparametric Element. In applying the finite element technique the mass is divided into a discrete number of elements small enough in size to insure satisfactory accuracy (Fig. 1). The soil continuum (such as the soft clay and aggregate in a haul road) is modeled by an eight node, isoparametric element. This element has the capability to model curved boundaries and has a quadratic variation of displacement. The stiffness of each isoparametric eight node element is obtained by integration using nine sampling points.

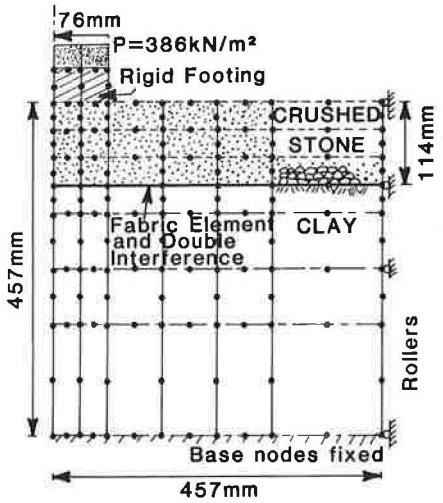

Fig. 1 Typical Finite Element Used to Model Laboratory Tests.

Nonlinear and Large Displacement Analysis. The solution strategy for nonlinear and large displacements is based on the solution of incremental formulations of the problem. A stress dependent elastic modulus E can be used having the form (1) $E = K\sigma_\theta^n$ where K and n are material properties and σ_θ is the sum of the principal stresses or (2) $E = f(\sigma_1 - \sigma_3)$ where σ_1 and σ_3 are the major and minor principal stresses, respectively. Load is applied to the model in small increments, and computations of incremental and total stresses are performed by solving a system of linear, incremental equilibrium equations for the system. Both geometric (large displacements) and material nonlinearities can be included as desired in the formulation. Geometric nonlinearities are caused by the change in geometry of the body as it undergoes large displacements.

Using the large displacement option the updated Lagrangean approach (1,6) is employed in the analysis. This formulation considers the change in geometry of each element with each load increment. Stresses, strains, and displacements are referred to the immediately previous configuration of the body. Unbalanced forces are reversed and applied to the nodes after each iteration.

No-Tension Analysis. The no-tension analysis considers the inability of granular, cohesionless materials such as crushed stone to take tension. These materials have no true cohesion and can take only limited amounts of tension in the horizontal direction due to interlock, friction and passive soil resistance outside the loaded area. A wheel loading causes relatively large vertical stresses which force the grains together at point contacts. Because of these normal stresses the granular material can take some friction before a tensile failure occurs (3). Special consideration must therefore be given to the bottom portion of a granular layer placed above the fabric in a haul road because of the existance of a tensile state of strain.

An attempt was made to extend the no-tension analysis for rock joints by Zienkiewicz, et al. (4) to the soil-fabric problem. Slow convergence of the technique was observed, with seven iterations per load increment not being sufficient to equilibrate the system even at low stress levels. The Zienkiewicz approach was therefore abandoned after several attempts to adapt it, and subsequently the simplified method for handling tension of Raad and Figueroa (5) was successfully implemented.

The principal stresses and strains are computed using GAPPS7 for each of the 9 integration points of the eight node isoparametric element used to model the granular material. The existance of failure is checked at the end of each iteration at each sampling point. To define failure the extended Drucker-Prager failure criteria (1,6) is used as a three-dimensional extension to the Mohr-Coulomb failure law for axisymmetric conditions. In apparent contrast to the Raad and Figueroa's approach, plastic strains are accumulated during the analysis.

This admittedly empirical approach for handling tension is illustrated in Fig. 2 for one stress condition. Assume the granular material is at a state of failure due to low lateral confining pressure, σ_3, at any one of the integration points as shown by Mohr circle C in Fig. 2. At failure the Mohr circle must just touch the failure envelope and cannot extent beyond it. Therefore, when the calculated failure circle extends beyond the envelope it is pushed back to just touch the envelope keeping σ_1 the same. Equilibrium of the system is checked after each iteration. After the modification the principal stresses comply with Mohr-Coulomb failure criteria, and the material will be in a perfectly plastic failure state. Use of small load increments produces stress states that

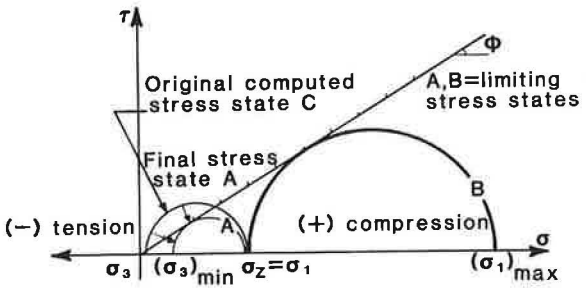

Fig. 2 Approximate No-Tension Correction Used in Aggregate.

are close to the failure envelope and hence only require a small amount of correction.

Interface Element. Slip between the fabric and adjacent material is of considerable interest in studying the behavior of fabric reinforced solids. Special elements illustrated in Fig. 3 were therefore developed to model the fabric interfaces using the work of Wilson, Goodman, Herrmann and others (1). In the figure two interface elements are shown on each side of four fabric elements.

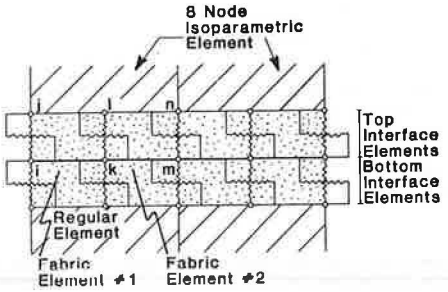

Fig. 3 Soil-Fabric Finite Element Model.

The interface elements are also attached at the common nodes to the isoparametric elements. The interface element ijklmn (Fig. 3) is formed by six linear springs and six nodes, and satisfies compatibility requirements with adjacent eight-node elements. In the model the concentrated normal and shear springs replace the uniformly distributed foundation type modulus, k, which is the ratio of stress divided by the displacement.

The computed shear and normal stresses at the interface define the mode of behavior along the interface: no slip, slip, or separation. Depending on the behavior mode, the actual forces developed at the interface are applied to the system. The maximum allowable shear at the interface is given by the Mohr-Coulomb Failure Law

$$\tau_{max} = c_a + \sigma_n \tan\delta \qquad (1)$$

where:

c_a = adhesion between the interface materials

δ = friction angle between the interface materials

σ_n = normal stress to the interface

The interface material properties c_a and δ have been determined in the laboratory by performing dynamic, direct shear tests simulating the fabric-soil interface. If the shear strength of the material in contact with the fabric is less than the adhesive strength given by Eqn. (1), (which in general was found not to be true in the tests performed) the soil shear strength controls along the interface.

Fabric Element. The fabric element (Fig. 3) models the reinforcing fabric placed for a haul road application between the aggregate and subgrade. Linear, two-dimensional, axisymmetric and plane strain fabric elements were developed as extensions of a one-dimensional pinned end bar element. To give a good approximation of the behavior of the interface and the fabric, two fabric elements are placed adjacent to one interface element (Fig. 3). The fabric element can only take tension in the plane of the fabric; compression and bending is not permitted. As a result, the fabric element when carrying a tension load must remain straight between node points. Since small fabric elements are used, a good approximation is obtained to the curved profile actually assumed. The friction forces that are developed along the fabric are applied at the nodes of the element. In application the fabric-interface model has been found to give quite good results. As the load is increased in increments and iterations are carried out, a nonlinear fabric load-deflection curve can be followed in the analysis.

Solution. The stiffness of the system is determined by adding the stiffness contributions from the isoparametric, interface and fabric elements. Using the applied loads and system stiffness, the linear equations of the system are solved using an efficient, narrow banded equation solver (6). The stiffness of the system is varied after each load increment and iteration. This requires extra computer time to form the stiffness matrix for each load increment and iteration, but reduces considerably the number of iterations for convergence in a nonlinear analysis. By varying the system stiffness in this manner, a closer representation of the constitutive equations is obtained when slip, tension, and yield occur.

MODEL TESTS

A laboratory program was developed to experimentally examine under conditions of repeated loading the structural response of aggregate-soil (AS) and aggregate-fabric-soil (AFS) systems. An important secondary purpose of the test program was to aid in the validation of the GAPPS7 program. Haul road type systems consisting of soft subgrade soil, fabric and crushed stone were modeled in two circular test tanks. Measurements made during the repeated loading included permanent deformations throughout the section (including surface rutting), vertical and horizontal stresses and a limited number of fabric deflection strain) measurements.

Test Pit Construction and Loading. An extensive test program was performed in a 0.9 m dia. (3 ft.) pit to establish relationships between rut depth, aggregate thickness, and subgrade strength. A large 2.5 m (8 ft.) dia. pit was used for a limited number of tests. This size test facility permitted using an aggregate layer thickness and loading representative of conventional haul roads. One purpose for this latter series of experiments was to provide a scale factor for the results obtained from the smaller scale tests.

A soft clay subgrade (CL by the Unified Soil Classification System) was constructed having a 21 to 62 kN/m^2 (3 to 9 psi) undrained strength in the small pit and about 28 kN/m^2 (4 psi) in the large pit. The clay was thoroughly blended with the desired amount of water and then placed in uncompacted lifts of about 50 mm (2 in.) thickness in the small pit and 100 mm (4 in.) in the large pit, and then compacted. The moisture content, which varied from about 19.5 to 23%, was adjusted to achieve the desired subgrade strength. A subgrade thickness of 760 mm (30 in.) was used in all tests in the large pit; a 380 mm (15 in.) thick subgrade was used in the small pit.

For tests using fabric, a circular piece larger than the test pit was cut and placed on the subgrade with the excess material being turned up at the pit wall. The fabric used in this study was a nonwoven, heat bonded polypropylene manufactured by DuPont and sold under the trade name of Typar® ★ spunbonded polypropylene, Style 3401.

A crushed, dense-graded granite aggregate having a 25.4 mm (1 in.) maximum size was then placed in loose lifts of 50 to 75 mm (2 to 3 in.) and thoroughly compacted. For the 2.5 m (8 ft.) pit, a 370 mm (14.6 in.) thick aggregate layer was used while for the 0.9 m (3 ft.) pit, layer thicknesses of 150, 190 and 230 mm (6, 7.5, and 9 in.) were used. The repetitive load was applied to the surface of the crushed stone through a 300 mm (12 in.) dia. rigid plate for the large pit; a 150 mm (6 in.) dia. rigid plate was used for the small pit. In both cases 20 repetitions of a haversin shaped load pulse was applied per minute to the top of the rigid loading plate using a pneumatic or hybrid pneumatic-oil loading system. The dynamic load pulse had a duration of 0.2 sec. and a peak pressure of 482 kN/m^2 (70 psi).

Typical measured rutting as a function of the number of load applications obtained from the 0.9 m (3 ft.) dia. test pit is illustrated in Fig. 4. The surface deformations (rutting) shown in this figure was measured using dial gages. This figure shows that the use of the Typar® fabric has an important beneficial effect upon reducing rutting.

Pressure and Plastic Strain Measurements. Small pressure cells utilizing a special diaphram wire resistance strain gage were used to measure the pressures within the soft clay subgrade. Details of cell construction, calibration and placement are given elsewhere (7). The pressure cells were offset 75 mm (3 in.) in the small pit from the load centerline, and placed at depths of 38, 89, 150, 216 and 279 mm (1.5, 3.5, 6, 8.5, 11 in.) below the top of the subgrade. Pressure cell readings were taken during application of the repeated loading. Final cell locations and orientations were carefully determined after completion of each test. The vertical pressures measured in the large pit are summarized in Table 1 (including location) and were obtained for surface rut

★ Registered Trademark of the DuPont Company.

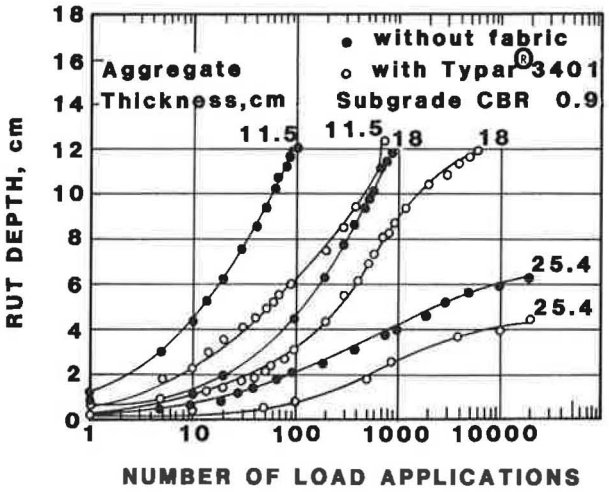

Fig. 4 Rut Depth as a Function of Applications With and Without Fabric: 0.9 m Test Pit.

depths of about 70 to 100 mm (3 to 4 in.).

Vertical plastic strains within the soft clay subgrade were determined for selected tests in the 0.9 m (3 ft.) pit using 19 Bison sensors (7). Vertical stacks of strain sensors were placed at 16 mm (4 in.) intervals going from the centerline out to 63 mm (16 in.). The typical variation of plastic strain in the subgrade on the centerline of the load is shown in Fig. 5 for a similar system with and without fabric. A significant reduction in plastic strain was found to occur immediately below the fabric along the centerline.

DISCUSSION

Stress Distribution. The GAPIN Program indicates as shown in Fig. 6 a reduction of 8 to 14% in vertical stress along the centerline for systems reinforced with Style 3401 Typar® compared with nonreinforced systems. Stress distributions measured in both test pits also show similar important stress reductions in fabric reinforced systems.

Figure 7 shows the measured variation of vertical stress along the centerline as a function of depth for pressure cells 3, 7 and 9 in the large pit. The systems reinforced with fabric showed approximately a 20% reduction in stress in the soft clay along the centerline compared to the AS systems. At the crushed stone-clay interface the vertical stress in the fabric reinforced systems was slightly less than Boussinesq stress distribution theory for a homogeneous elastic continuum. With increasing depth the measured stresses were greater than Boussinesq in this test series. The rigidity of the bottom of the tank was at least partly the cause of the increase in the measured stresses. Pressure cell 5, offset 460 mm (18 in.) from the load centerline and 150 mm (6 in.) below the top of the subgrade, showed greater vertical stresses for the AFS system than for the AS system (Table 1). Subgrade profile measurements made after the test showed this cell was directly below the approximate location of maximum subgrade heave. The GAPPS7 program also indicates a slight increase in pressure in the heave zone, although not as great as measured. The program also indicates the stress redistribution is caused by (1) plastic flow of soil beneath the originally more highly stressed center area resulting in softening of the clay and (2) the downward membrane effect due to in-plane fabric stress.

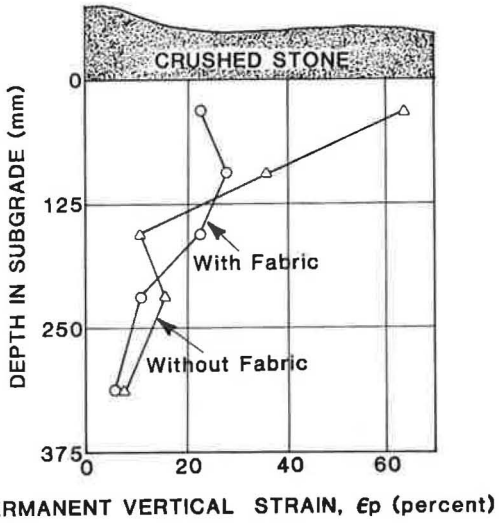

Fig. 5 Permanent Vertical Compressive Subgrade Strain Observed as a Function of Depth in the Subgrade: 0.9 m Pit Tests.

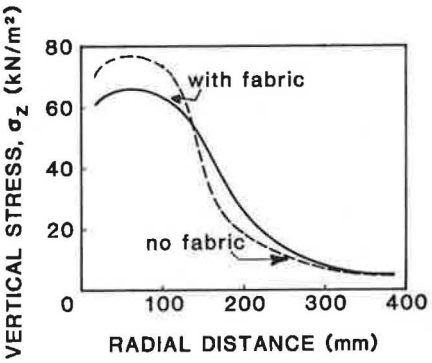

Fig. 6 Vertical Stress on a Horizontal Plane Computed by GAPPS7 (Mesh Shown in Fig. 1).

Table 1. Stresses Measured by Pressure Cells in 2.5 m Pit Tests.

Cell No.	Initial Position		Stress Normal Pressure Cell (kN/m²)	
	Depth (mm)	Offset (mm)	With Style 3401 Typar®	Without Fabric
9	406.	0	82.7	107
3	508.	0	75.8	107
4	762.	0	-	-
7	1070	0	37.9	44.8
8	508.	152.	56.5	85.6
6	508.	305.	48.2	51.7
5	508.	457.	11.0	5.5
2*	406.	457.	23.4	34.5
1*	813.	762.	23.4	23.4

*Radial stress - all other stresses are vertical (25.4 mm = 1 in.; 6.89 kN/m² = 1 psi).

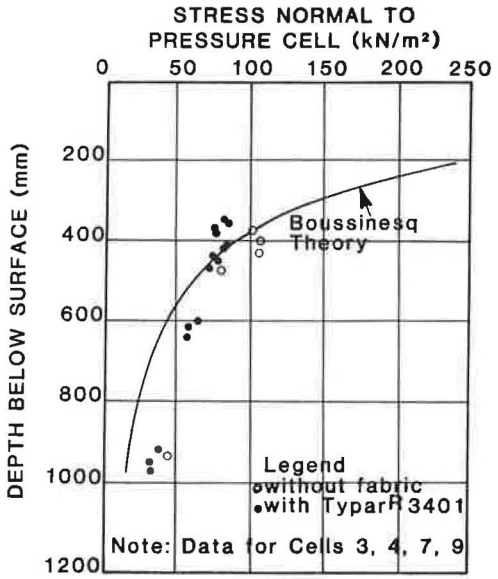

Fig. 7 Measured Stress Under Load Centerline in Subgrade of 2.5 m Pit Test.

Pressure cell measurements made in the small pit indicate: (1) prior to substantial rutting, the measured stresses in both AFS and AS systems averaged about 90.5% of that predicted by Boussinesq theory; less than 2% difference was observed between the two systems; (2) after substantial surface rutting (7 to 10 cm or 3 to 4 in.), the measured stresses for the AFS systems averaged about 83% of Boussinesq values compared with 88% of Boussinesq stresses in the AS system. In each case the changes of cell location and orientation were considered in the comparisons. The GAPIN program gave, for the fabric reinforced systems and moderate rut depths, vertical centerline stresses corresponding to about 80% of Boussinesq stresses in the subgrade.

Permanent Deformation. Beneath the repeated loading the model tests show the aggregate pushes downward into the subgrade causing the clay to flow laterally outward and upward. This lateral flow results in a radially offset bulge (heave) on the surface. As the thickness of the aggregate increases, the depth of subgrade rutting and height of heave both decrease, while the width of the rutted area increases. Use of Style 3401 Typar® was found to have a similar effect on rut development as increasing the aggregate layer thickness.

AFS systems, reinforced with this fabric, exhibited up to three times more vertical plastic strain in the aggregate at failure than did nonreinforced systems having similar surface rutting. This trend was most pronounced in the weaker systems. The number of repetitions to cause the same magnitude of rutting in the AFS systems, however, was much greater than in the AS systems. In the AFS systems the greatest amount of plastic vertical strain occurred in the aggregate layer, while in the AS systems the greatest plastic strain occurred in the clay.

Fig. 8 shows the experimental relationship between the amount of densification (volume change) and shear (distortion) occurring in the soft clay subgrade for both AFS and AS systems. As the initial stress ratio increases, the importance of shear distortion rapidly increases in both type systems, accounting for about 50% of the subgrade rutting at the stress ratio of 3 and about 75%

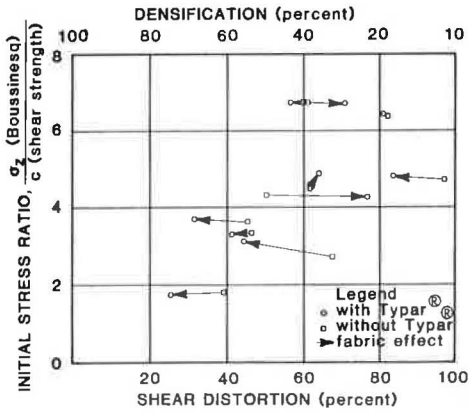

Fig. 8 Amount of Shear Distortion and Densification in Subgrade as a Function of Initial Stress Ratio.

at a stress ratio of 5. The stress ratio is defined as the vertical Boussinesq stress divided by the subgrade shear strength. These findings are quite reasonable since densification in the soft clay occurs gradually under the application of a large number of load repetitions as the water is slowly squeezed from the clay. Therefore, either AFS or AS systems subjected to a high initial stress ratio undergo a shear distortion type failure before densification can become the dominating mechanism.

Use of the fabric causes a substantial reduction in permanent strain (and hence rutting) in the soft clay subgrade for a depth equal to about one loading diameter B beneath the interface (Fig. 5). This reduction in strain decreases almost linearly with depth. Further, the maximum vertical plastic strain in systems containing fabric occurred at a depth of about 0.6B beneath the interface. In systems without fabric, the maximum strain occurred at or very near the interface and generally decreased with increasing depth. Due to application of a heavy wheel loading, the soft clay just below the crushed stone is stressed to a high percent of its shear strength. As a result, the relatively small reduction in stress which occurs when the fabric is present causes an important reduction in the accumulation of permanent strain in the zone just below the fabric as shown in the model tests.

Fabric-Interface. The variation of strain in Style 3401 Typar® fabric with stone thickness and rut depth obtained using the GAPPS7 program is shown in Fig. 9. The GAPPS7 program indicated excessive rutting would develop before 700 repetitions for an aggregate thickness of 330 mm (13 in.). As this system approached an excessive rutting condition, the calculated maximum fabric strain was 3% at the centerline and 2% at a radial distance from the centerline of 1.33B, where B is the diameter of the load. The fabric strain measured in the small pit for a rut depth of 76 mm (3 in.) and radial offset distance of 1.33B was 1.9%; this value compares quite favorably with the theoretical value of 2%. These results indicate that the Typar® fabric is stressed to about the elastic limit which corresponds to 3.2 N/mm (18 lb./in.). This stress level is in a safe working range well below the ultimate value of about 7.4 N/mm (42 lb./in.).

Using measured interface friction and adhesion properties, the GAPPS7 program indicates slip does not occur for AFS systems which are adequately designed having a subgrade shear strength as low as 22.7 kN/m^2 (3.3 psi); lower strengths have not been investigated. As large rut

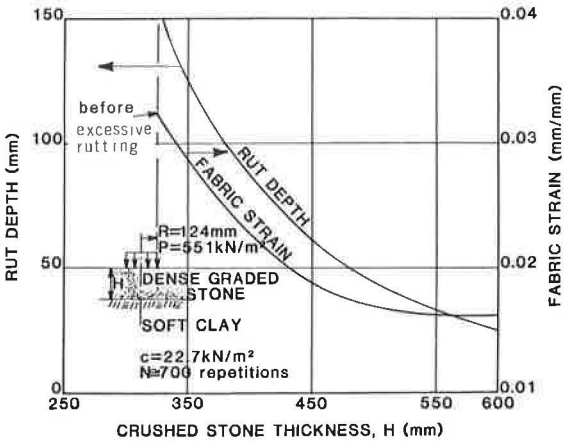

Fig. 9 Variation of Rut Depth and Fabric Strain as a Function of Crushed Stone Thickness.

depths develop, however, slip between the clay and fabric can occur at least at some locations.

General. The test results show for a given system with or without fabric, a threshold thickness of crushed stone exists which separates a stable system having tolerable levels of rutting from an unstable system. This threshold stone thickness is less for AFS systems than for AS systems (Fig. 4). For overstressed systems having crushed stone thicknesses less than the critical value, rapid accumulation of large rutting in the subgrade is primarily due to shear distortion (flow) of the subgrade laterally from beneath the load.

These results clearly indicate that Style 3401 Typar® is effective in changing the state of stress and strain in the subgrade. As rutting increases, vertical and radial stress under the loaded area are reduced while the vertical compressive stress outside the loaded area (in the region of subgrade heave) is increased. The reduced stresses observed are most likely due to (1) upward induced stress (membrane effect) and possibly (2) greater aggregate modulus (as a result of confinement/ reinforcement provided by the fabric). This alteration in state of stress is a primary reason that the fabric reinforced system exhibits greater rutting resistance.

The substantial alteration of plastic strain distribution in the subgrade is very interesting and obviously has a major impact on system rutting. The reduction of vertical plastic strain in the subgrade for systems containing fabric apparently is due at least in part, to the reduced vertical compressive stresses. However, the reduced vertical stresses do not explain why the vertical plastic strain in the soil adjacent to the fabric is less than that a few centimeters down into the subgrade. This anomaly is most likely caused by (1) the increased confinement offered to the soil adjacent to the fabric and (2) reduced shear stresses at the surface of the subgrade.

CONCLUSIONS

Both the model tests and the GAPPS7 program show the presence of fabric causes a definite beneficial alteration of the stress and plastic strain distribution in a fabric reinforced haul road type system. The laboratory model tests and the GAPPS7 computer program offer a sound mechanistic approach for studying the behavior of fabric reinforced systems and developing useful design relationships. The GAPPS7 program was recently developed and application of this powerful tool is just being implemented.

ACKNOWLEDGEMENTS

This research was sponsored by E.I. DuPont de Nemours & Company in cooperation with the School of Civil Engineering, Georgia Institute of Technology. The continuing help of Dr. Lee Murch and Mr. Richard Weimar, Jr. of DuPont is gratefully acknowledged. Appreciation is also expressed to the many graduate and undergraduate students who greatly contributed to this study including Bill Schauz, Alan Stensland, Keith Bennett, David Langford, Bob Chambers, and K. Molavi.

REFERENCES

(1) Zeevaert, A.E., Finite Element Formulation for the Analysis of Interfaces, Nonlinear and Large Displacement Problems in Geotechnical Engineering, PhD Thesis, Georgia Institute of Technology, Atlanta, Ga., 1980.

(2) Zeevaert, A.E., and Barksdale, R.D., Users Manual, Finite Element Program for the Analysis of Geotechnical Problems, GAPPS7, School of Civil Engineering, Georgia Institute of Technology, Atlanta, Ga., 1981.

(3) Barksdale, R.D., "Compressive Stress Pulse Times in Flexible Pavements For Use in Dynamic Testing", Highway Research Board, Record No. 345, 1971, pp.32-44.

(4) Zienkiewicz, O.C., Best, B., Dullage, C., and Stagg, K.G., "Analysis of Nonlinear Problems in Rock Mechanics with Particular Reference to Jointed Rock Systems", Proceedings, Second International Conference in Rock Mechanics, Yugoslavia, 1970, pp. 8-14.

(5) Raad, L., and Figueroa, J.L., "Load Response of Transportation Support Systems", Transportation Engineering Journal, ASCE, TE1, January, 1980, pp. 111-128.

(6) Bathe, K.J., Wilson, E.L., Numerical Methods in Finite Element Analysis, Prentice Hall, 1976.

(7) Intraprasart, S., Experimental Studies and Analysis of Compacted Fills Over Soft Subsoils, PhD Thesis, Georgia Institute of Technology, Atlanta, Ga., 1979.